Innovation in Computational Structures Technology
B.H.V. Topping, G. Montero and R. Montenegro, (Editors),
Saxe-Coburg Publications, Stirlingshire, Scotland, 888-888.

Chapter 0123456789

Adaptive Impact Absorption

J. Holnicki-Szulc, G. Mikulowski, A. Mroz and P. Pawlowski
Smart-Tech Centre
Institute of Fundamental Technological Research
Warsaw, Poland

Abstract

The approach proposed in this paper, in contrast to the standard passive solution, focuses on *active adaptation* of energy absorbing structures (equipped with sensor system detecting, identifying the impact in advance, and controllable semi-active dissipaters) with high ability of adaptation to extreme overloading. The paper presents a concept of m*ulti-folding structures* providing the additional value of energy dissipation, due to the synergy of repetitive use of active elements (equipped with so-called structural fuses), according to pre-designed optimal distribution of yield stress levels, triggering the desired sequence of local collapses.

The second example, an *adaptive wind turbine*, demonstrates the idea of controlling the value of peak dynamic force that is transferred to the support by means of a pneumatic system with a controllable on/off piezo-valve. An alternative for developing new blade materials is to introduce a semi-actively controlled connection between blade and hub with controllable characteristics.

Finally, the paper discusses the possibility of real-time, dynamic mass identification, which is an important part of the process of load identification. Numerical simulations and experimental results are presented.

Keywords: adaptive impact absorption, controlled shock absorbers, optimal design, structural control, real-time load identification.

1 Introduction

Motivation for the undertaken research is in response to the requirement for high impact energy absorption in areas such as: structures exposed to risk of extreme blast and light; thin-walled tanks with high impact protection; vehicles with high crashworthiness; protective barriers. Typically, the suggested solutions focus on the design of passive energy absorbing systems. These systems are frequently based on the aluminium and/or steel honeycomb packages characterised by a high ratio of

specific energy absorption. However high the energy absorption capacity of such elements they still remain highly redundant structural members that do not carry any load in an actual operation of a given structure. In addition, passive energy absorbers are designed to work effectively in pre-defined impact scenarios. For example, the frontal honeycomb cushions are very effective during a symmetric axial crash of colliding cars but are completely useless in other types of crash loading. Consequently, distinct and sometimes completely independent systems must be developed for specific collision scenarios.

In contrast to the standard passive systems (see advanced methodologies of computer simulation and design for improved crash-worthiness, References [1]–[6]) the proposed approach focuses on *active adaptation* of energy absorbing structures (equipped with sensor systems detecting and identifying impact in advance and controllable semi-active dissipaters, so called *structural fuses*) with a high ability to adapt to extreme overloading [7]. The following characteristic cases of adaptive impact absorption (AIA) problems can be identified:

- the case of a protective structure (for example, a protective barrier) sustaining impact overload with minimised maximum acceleration (or force)
- the case of an adaptive structure sustaining impact overload with minimum global measure of plastic-like distortions generated in adaptive dissipaters during the impact scenario

The first case corresponds to smoothing down the impact effect (such as for reduction in fatigue effect, as in adaptive landing gear [13]) and coming from service loads, while the second one corresponds to the impact absorption (for example, from critical environmental loads) with minimal cost of induced distortions. In both cases a semi-active or fully active solution can be applied depending on constant or time-dependent modifications realised via controllable dissipative devices. **Note, these devices are dissipaters (with no need for an significant power supply) rather then actuators**. Feasible, dissipative devices (*structural fuses*) under consideration in the application discussed below can be based on the following technologies:

- adaptive dissipaters based on MR fluids
- adaptive dissipaters based on (hydraulic or pneumatic) piezo-valves
- adaptive dissipaters based on SMA alloys

The present paper demonstrates progress in the AIA research field obtained recently in our research group and is based on the following previously published conference contributions, References [8]-[11]. The monograph, Reference [12], under preparations, will soon present more detailed discussion of the problems under consideration.

2 The concept of the adaptive multi-folding microstructure

The objective of this section is to propose a new concept of adaptive microstructures with high energy absorbing characteristics. Let us discuss the truss-like micro-

structure (similar to a honeycomb layout) shown in Figure 1 equipped with specially designed micro-fuses, for example, Figure 2a, with stacked thin washers made of shape memory alloys (SMA) as controllable stickers, Figure 2b. The micro-structural response to external loading strongly depends on the yield stress levels applied to micro-fuses and these levels can be controlled by activating proper numbers of SMA micro-washers in each sticker.

The crucial point for obtaining additional energy dissipation value (due to the synergy of the repetitive use of dissipaters) is to pre-design the optimal distribution of yield stress levels in all stickers, triggering the desired sequence of local collapses. Let us call the discussed adaptive microstructure the a*daptive multi-folding microstructure* (MFM).

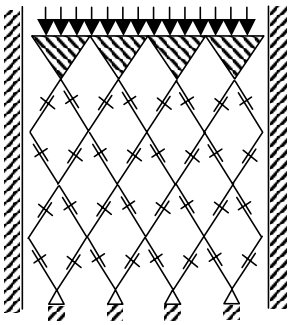

Figure 1: Truss-like microstructure

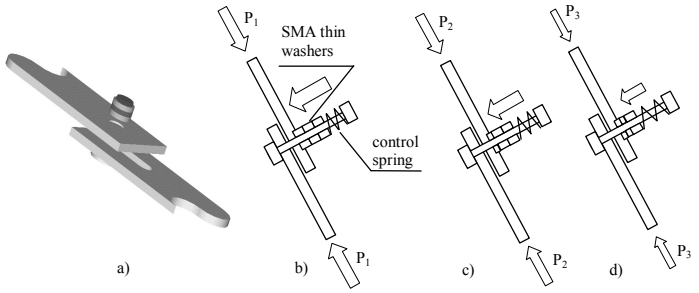

Figure 2: Controllable micro-stickers

To analyse the performance of the proposed microstructure, let us follow the response of the model shown in Figure 3, corresponding to the behaviour of one column of the discussed hypothetical smart material.

Assuming idealised truss structure model (Figure 3a) is composed of perfect elastoplastic members with the yield stress levels shown (obtained by properly activated fuses), the sequence of collapse is shown in Figs 3b, 3c and 3d, respectively. When compressing forces in all members of the idealised truss-like structure shown in Figure 3a are the same, all members with the stress limit level σ_2 start to yield first, converting the structure into the configuration shown in the Figure 3b. Then the yield stress level for elements marked σ_3 is lower than for tripled elements (with a stress limit of $2\sigma_1$-δ) and the consequent structural configuration is that shown in Figure 3c. Following the same procedure the next configurations, that is, Figure 3d and Figure 3e can be reached.

The piece-wise linear constitutive model of MFM (applicable in computational simulations), shown in Figure 4, can be proposed. Cyclically loaded and unloaded adaptive members will have their characteristics with high hysteresis (Figure 4b). Additionally, fictitious members (dotted lines in Figure 4a) with piece-wise linear locking properties (Figure 4c) are proposed to model contact problems in the loading scenario. The numerical model for simulation of MFM performance will be required to take into account both physical and geometrical non-linearities.

Note that the resultant characteristic (Figure 3f) of the MFM model is not unique. The final shape of this curve can be modified according to our requirements by changing the yield stress level distribution.

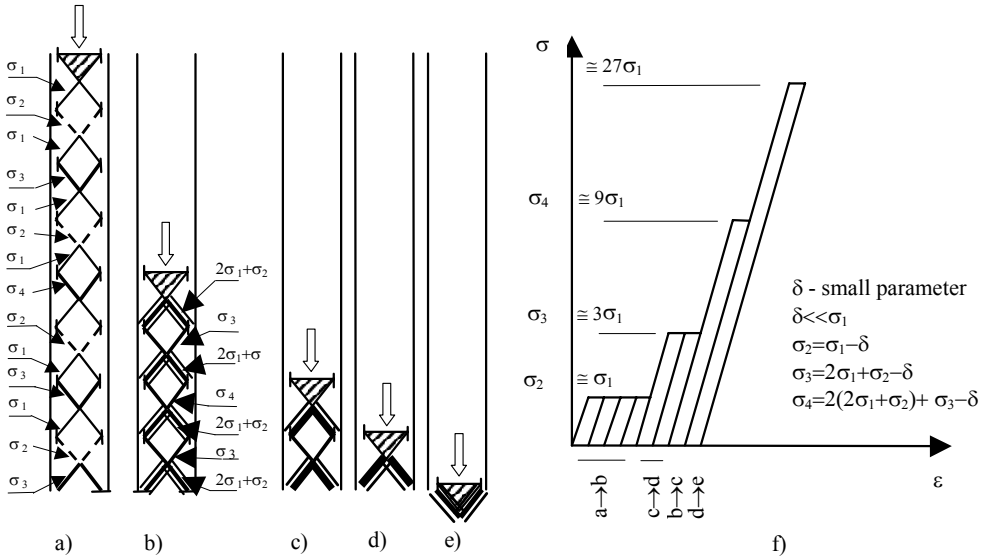

Figure 3: Model of an adaptive multi-folding microstructure (MFM)

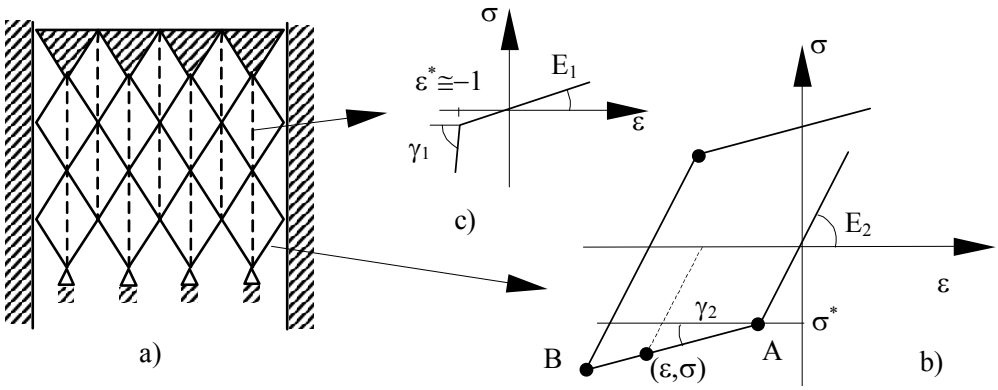

Figure 4: Constitutive model of the micro-structure

2.1 Optimal control

To provide optimal energy absorption it is necessary for the microstructure to perform a process of adaptation consisting of three stages:

- Load identification
- Choosing optimal strategy
- Structural adaptation

The dynamic load level can be evaluated prior to an impact by measuring velocity and estimating the mass of a colliding body. Alternatively its value might be identified at the beginning of impact by structural loading sensors. In order to dissipate the kinetic energy in an optimal way, one has to apply correct strategy to active elements of the microstructure. Two strategies of the structural control are formulated:

- semi-active control
- real-time control

In the first case pre-selected triggering stress levels σ_i in structural elements remain unchanged during an impact, in the second, the theoretical possibility of real-time changes in control parameters is assumed. Although full real-time control does not seem to be feasible in a real design, one can expect at least a few stress changes during the impact time might be applied.

The problem of optimal control can be formulated as follows:

Semi-active control - for a given impact load minimise the difference between acceleration values in selected points of the structure and desired response function $\ddot{q}_i^d(t)$:

$$\min \quad U^0 = \sum_t \sum_i \left[\ddot{q}_i(t) - \ddot{q}_i^d(t) \right]^2 \tag{1}$$

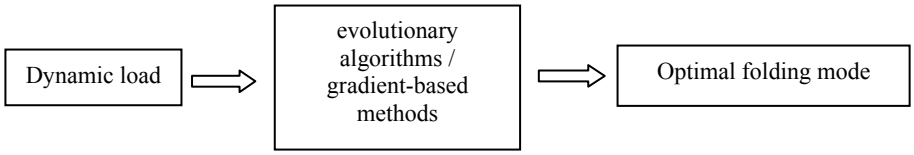

Figure 5: The algorithm searching for maximum load level, safe for adaptive MFM, semi-active control

Real- time control - for a given impact load, for every time step minimise the difference between acceleration values in selected points of the structure and desired response function $\ddot{q}_i^d(t)$:

$$\min \quad U^0(t) = \sum_i \left[\ddot{q}_i(t) - \ddot{q}_i^d(t) \right]^2 \tag{2}$$

subject to the following constraints

$$|\bar{\sigma}| \in \langle \bar{\sigma}_{\min}, \bar{\sigma}_{\max} \rangle, \qquad \max\{q\} \le \bar{q} \tag{3}$$

where $\bar{\sigma}$ denotes the plastic-like yield stress level and $\bar{q}$ is the maximum crush distance.
Satisfactory solution of the above problem exists if the external load intensity is not higher then the maximum safe load level. Beyond this, a limit control strategy with the highest possible capability for energy dissipation must be applied.

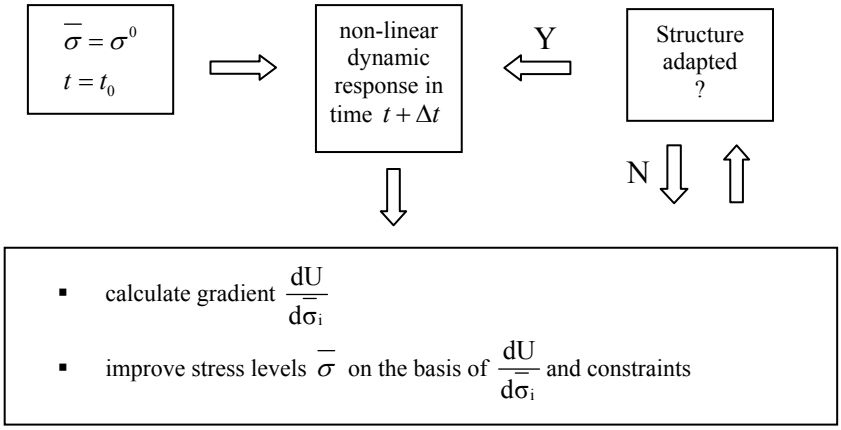

Figure 6: The algorithm searching for maximum load level, safe for adaptive MFM, active control

3 Numerical demonstrations of structural adaptation to impact loads

3.1 Multi-folding sections

A numerical model of the basic MFM demonstrator set-up (Figure 7) has been created and tested. The model consists of six elements with identical cross sections and elastic properties of the material. There are only two control stress levels σ_1 for lower and upper elements *"A"* and σ_2 for middle elements *"B"*. Admissible values of control parameters belong to a range $|\bar{\sigma}| \in \langle 4e8Pa, 8e8Pa \rangle$. Maximum crush distance must be less than 4*H*. Contact elements provide correct model behaviour. The structure was subjected to a dynamic load (concentrated mass with initial velocity $\dot{q}_0$) simulating an impact. Kinetic energy of the load was increased linearly by changing mass value from 100kg up to 240kg with constant velocity 15m/s.
The response of the modelled structure strongly depends on the relationship between parameters σ_1 and σ_2. Different, effective folding sequences are depicted in Figures 8 and 9. In the case of first folding mode, which provides a very smooth response σ_1 is lower than σ_2. The second one, with $\sigma_1 > \sigma_2$, gives maximum energy absorption capability.
The evolution of stress, strain and plastic distortion for selected element *"B"*, corresponding to the second folding mode 2 is shown in Fig 11. Evolution of elastic and plastic energy is presented in Figure 10.

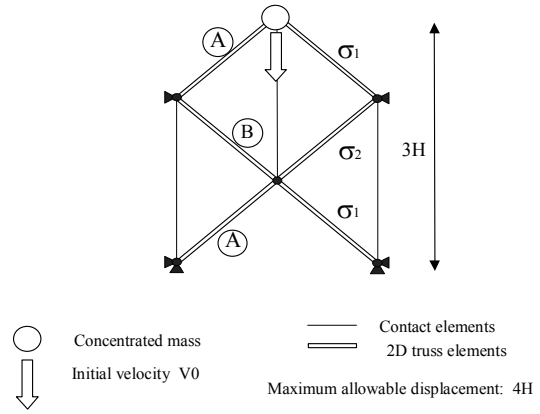

Figure 7: MFM demonstrator set-up

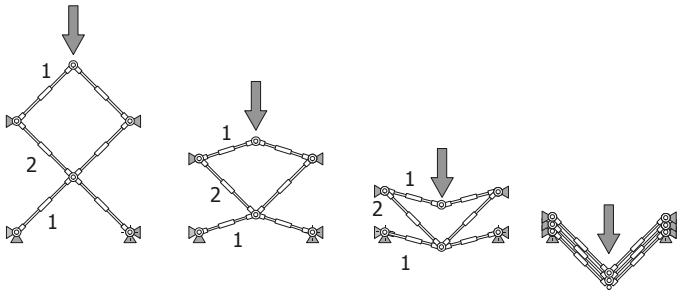

Figure 8: Folding mode one

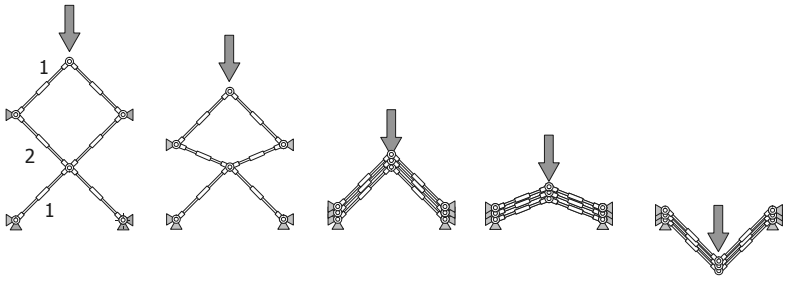

Figure 9: Folding mode two

In the numerical example only a semi-active control strategy was considered. Optimal distribution of control stresses in the structure with corresponding extreme acceleration values for the loaded node for different mass values are presented in figure 12. Note that at a kinetic energy value corresponding to mass of 130kg it is necessary to change folding mode form mode 1, which reached its limit load to mode 2. The results obtained are compared to the so-called *"passive absorber"* (the structure in folding mode 2 with the highest possible control stresses, providing extreme energy absorption).

Applied semi-active control gives a very stable response for different loading values combined with the possibility of a high reduction in acceleration level.

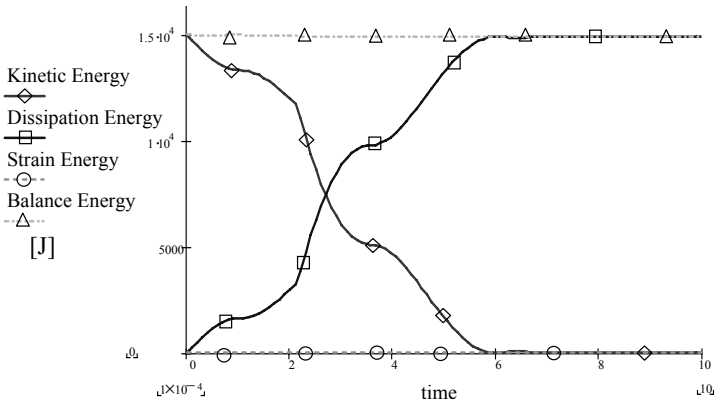

Figure 10: Evolution of energy components for dynamic response

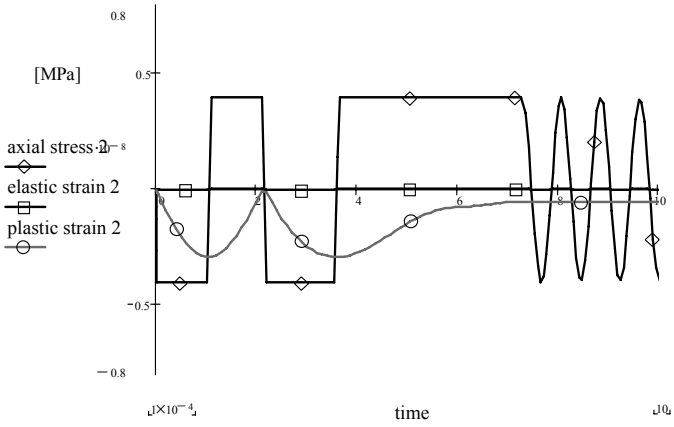

Figure 11: Evolution of stress, strain and plastic distortion for element *B*

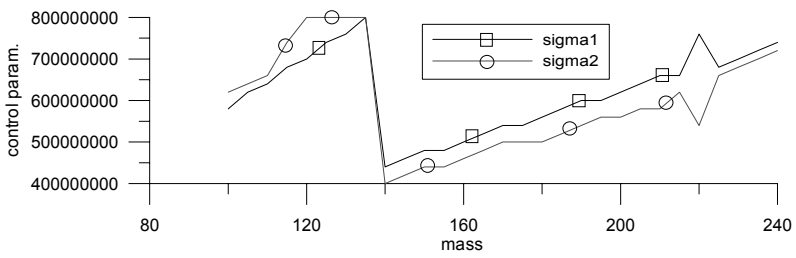

Figure 12: Optimal control parameters

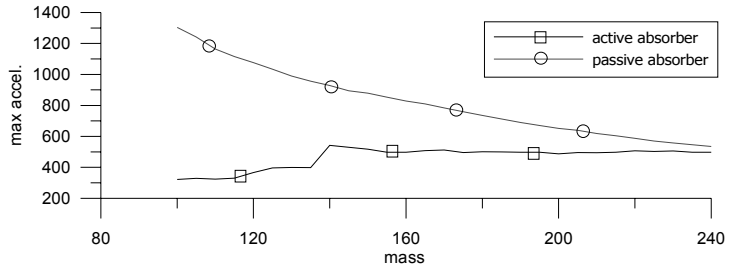

Figure 13: Objective function

The figures below present the evolution of acceleration and velocity of the absorber for the concentrated mass value of 100kg. A significant reduction of extreme acceleration and smooth velocity change in optimal solution is clearly visible.

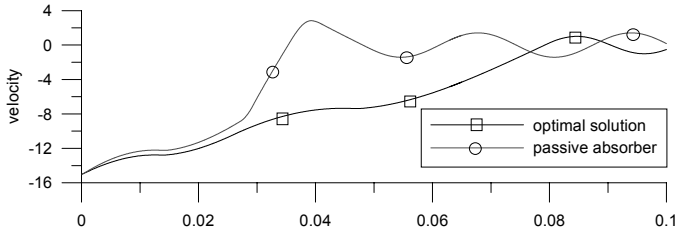

Figure 14: Evolution of velocity of the loaded node

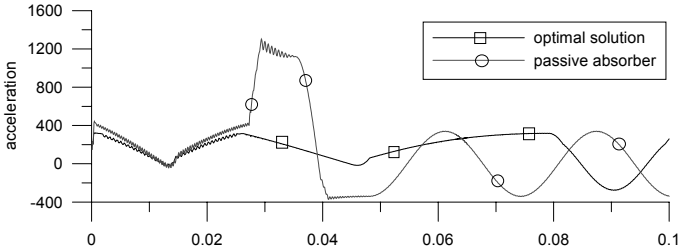

Figure 15: Evolution of acceleration of the loaded node

3.2 Adaptive tower

In order to minimise consequences of the dynamic load, a process of structural adaptation to an impact should be carried out. The process consists of the following, subsequent three stages:

3.2.1 Impact detection

Impact detection is provided by a set of sensors that respond in advance to a danger of collision such as radar and ultrasonic devices, or are embedded into the structure within a small passive crush zone (for example, piezo-sensors). Estimation of the impact energy is then based on an initial deformation of the passive zone.

3.2.2 Structural adaptation

The signal from the system of sensors must be directed to a controller unit, which selects an optimal distribution of yield forces P in active zones containing elements equipped with structural fuses. Figure 2 presents the concept of the fuse, consisting of a stack of thin, shape memory (SMA) alloy washers. The yield force in the active element depends on a friction force generated in the fuse by activating different number of washers. The initial value P_3 (without any activation) can be gradually decreased to P_2 and P_3 respectively, when one or two washers change their original shape. Due to the characteristics of the structural fuse, the active element can be modelled as elastic-perfectly plastic with a controllable yield stress value.

3.2.3 Self-repair (structural recovery)

Increasing requirements for structural durability and low-level operating costs create a need for new, smart solutions. The results of an extreme dynamic load may very often be fatal for a structure. In the case of structures equipped with active elements it is possible to remove residual distortions using low-level vibrations induced by an external or embedded shaker.

The following numerical example illustrates the concept of adaptive impact absorption. A 30m high tower, equipped with an active energy absorber, is considered as an example and depicted in Figure 16.

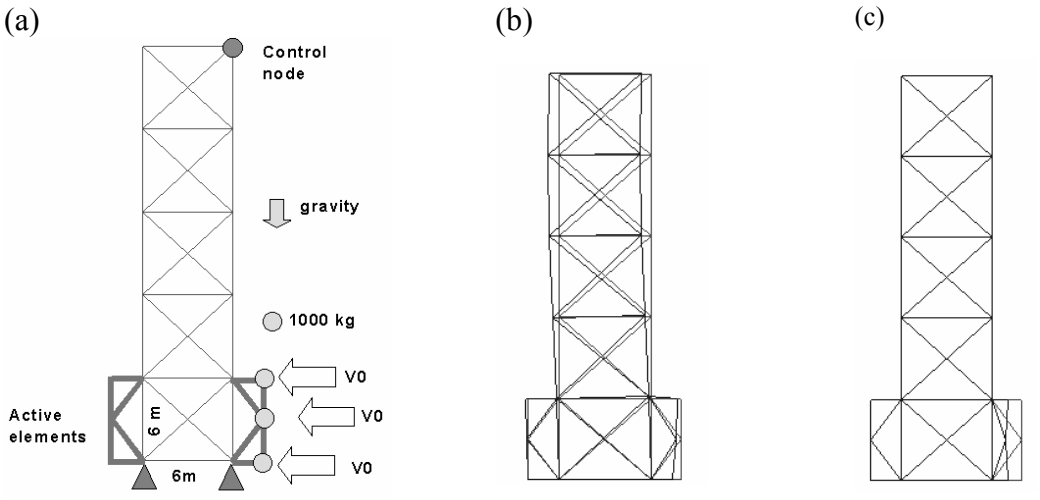

Figure 16: (a) Model of an adaptive structure (b) displacements of the elastic solution (scaled x 1.5) (c) displacements of the optimal solution

The structure is subjected to the impact of a mass of 3000kg with initial velocity of 8m/s. All structural members have a uniform cross-section area and elastic modulus. The yield stress level in active elements is adjusted according to the value of the kinetic energy of the impact, while in all passive elements it is equal to 6e8Pa. The

maximum allowable strain in controlled elements is constrained to 50% of their initial length.

The objective function of the optimisation problem is to minimise the horizontal acceleration of the controlled node at the top of the tower. Results for the problem for two different thresholds of yield stresses in active elements are presented in Figure 17. For the highest threshold of 6e8Pa the response of the structure is elastic while thresholds of 2.6e7Pa (the optimal solution) provide localised permanent plastic deformation. It is can clearly be seen that adaptive strategy provides a very significant reduction in the acceleration level and that control parameters in active elements should be adjusted according to the severity of the impact.

Two strategies of semi-active and active control might be considered. In the first strategy, yield stresses in structural members located in active zones remain unchanged during an impact. In the second one, a possibility of real-time changes in control parameters is assumed. The paper focuses only on the semi-active approach, which provides a good balance between expected results and complexity of control strategy.

A position of active elements follows from an assumption that only selected parts of the considered structure would be exposed to a danger of extreme, dynamic load. A number of active elements and their structural properties should be chosen as a result of the separate optimisation task.

The problem of the control may be formulated as follows: for a given structure and a given set of active elements $E_i \in A$, find optimal distribution of control yield stresses σ_i^p, minimising objective function f defined by the impact index I_2 (providing information about average acceleration level at monitored degrees of freedom (DOF) q_i^{cntrl}):

$$\min f(\sigma_i): \; f \to I_2 \tag{4}$$

$$I_2 = \frac{1}{T}\sum_{t=1}^{T}\sum_{i=1}^{Ncntr}\left|\ddot{q}_i^{cntr}(t)\right| \tag{5}$$

with the following constraints, imposed on control stresses and displacements in active elements:

$$\sigma_i \in \langle \sigma_{\min}, \sigma_{\max} \rangle \tag{6}$$

$$\max\left\{q_i(t) \in A\right\} \le q_i^{\max} \tag{7}$$

Two additional measures of structural dynamic response, describing overall acceleration level in the structure and maximum acceleration values at specified DOF, may be introduced:

$$I_1 = \frac{1}{T\,N}\sum_{t=1}^{T}\sum_{i=1}^{N}\left|\ddot{q}_i(t)\right| \tag{8}$$

$$I_3 = \max_{t,i}\{\left|\ddot{q}_i^{cntr}(t)\right|\} \tag{9}$$

where T is time of analysis, N is number of DOF, *Ncntr* is number of monitored DOF.

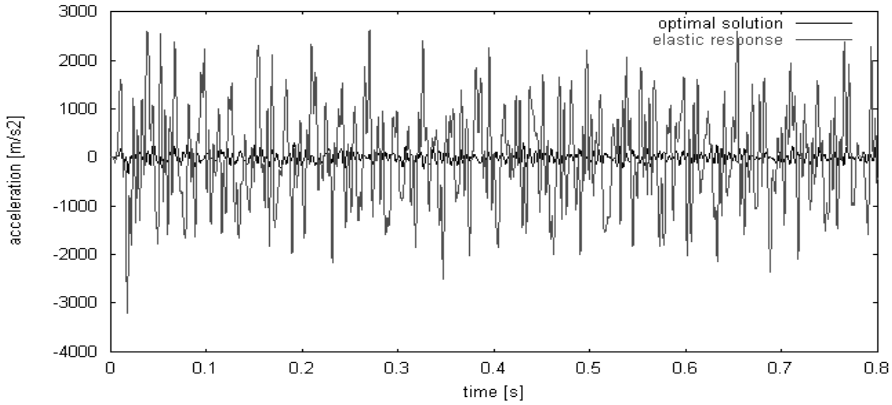

Figure 17: Horizontal acceleration of the monitored node, for the passive and the optimal plastic solution

After optimal impact absorption, permanent deformation is localised in selected active elements. Assume that residual strain in an active element is equal to ε_i^R. Low-level vibrations induced by a shaker (external or embedded into the structure) can generate strains $\varepsilon_i(t)$, which can be used to recover initial length. When residual and actual strains have opposite signs the structural fuse opens and releases accumulated distortions. In the case of equal signs, the fuse remains closed:

$$\sigma_i(t) = \begin{cases} \sigma^O \;\; if \;\; \varepsilon_i(t)\varepsilon^R < 0 \quad \sigma^O - open \\ \sigma^C \;\; if \;\; \varepsilon_i(t)\varepsilon^R > 0 \quad \sigma^C - closed \end{cases} \tag{10}$$
$$\sigma^C \gg \sigma^O$$

In order to ensure stability only one active zone should be recovered at a time.

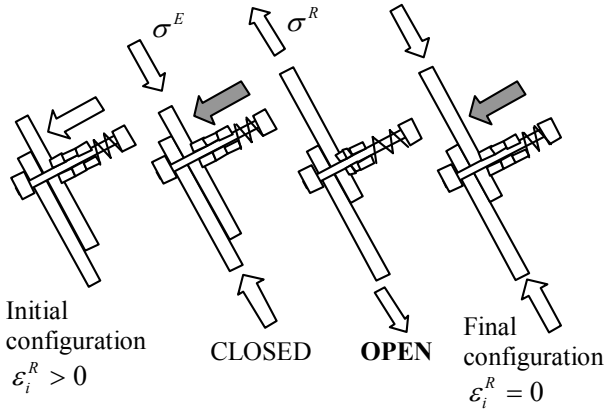

Figure 18: Structural fuse in recovery mode

4 Adaptive wind turbine

4.1 Motivations and the problem formulation

One of major technological limitations of up-scaling of modern wind turbines is the load bearing capacity of blade materials [14]. Connection between blade and hub has to withstand very large bending moments in particular during high winds. An alternative for developing new blade materials is to introduce a semi-actively controlled connection between blade and hub with controllable characteristics. This section demonstrates the idea of controlling the value of peak dynamic force that is transferred to the support by means of a pneumatic system with a controllable on/off piezo-valve. Pneumatic pistons, together with controllable valves, and pressure supply systems are used as smart actuators, typically as handling or positioning devices [15,16]. Contrary to applications in the present approach, pressure is withdrawn from the cylinder by using a smart valve and the whole system works in a semi-active way without applying external energy.

Piezo-materials are used in pneumatic systems either to allow for very fine positioning precision or as a piezo-actuator for micro-valve opening. Problems encountered for common pneumatic valves are long response times and, especially for low pressure, the need to use a pilot valve. In the present case the solution of a mechanically amplified piezo which drives the valve orifice means there is no need for pilot valve and the response time is of the magnitude of single milliseconds. In the first part of the section a numerical study is presented to demonstrate the idea and assess the effectiveness of solution. The experimental set-up is then presented.

The numerical model of the system consists of two major elements, that is, the slender, elastic part which can be viewed as a demonstrator ‘blade’ and a pneumatic piston which transfers the dynamic force to the support (Figure 19). The pneumatic spring, together with a controllable outlet, forms a ‘smart bond’ between the blade and the support. Further, it is assumed that the time it takes a high wind to develop is slow enough, so that the piston velocity does not exceed 1 m/s and the heating effects are negligible.

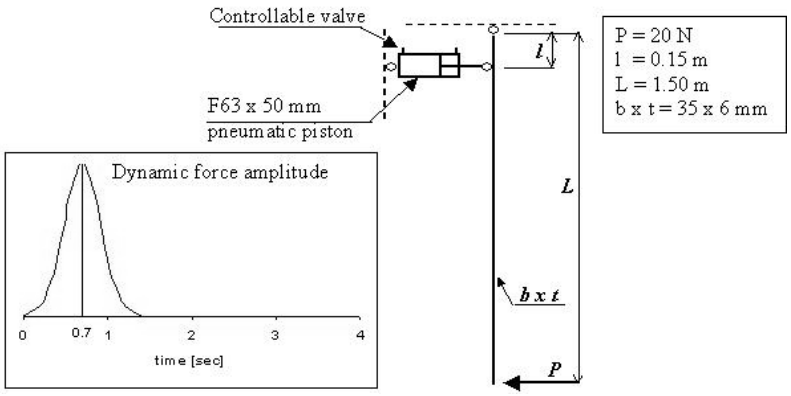

Figure 19: Numerical model features

Also, the working gas pressure in the cylinder should not exceed 1 MPa. Given the above, the process within the cylinder was assumed to be an adiabatic transformation of an ideal gas, at the constant temperature of T = 21ºC, according to the equation:

$$p \cdot V = n \cdot R \cdot T \tag{11}$$

It follows that the piston behaves like a non-linear spring with a hyperbolic characteristic. From the controllability standpoint it is preferable to use a piston with a big diameter due to the fact that given force could be obtained at smaller stroke and thus possibly a long stroke could be used during the active phase of the process. A ϕ 63 mm piston with the stroke of 50 mm was modelled in the simulation.

The simulation was performed with Abaqus/Standard code. The piston and remaining part of the pneumatic system were modelled with fluid cavity elements. Before adding control, results were compared with those obtained with non-linear Spring elements (Figure 20).

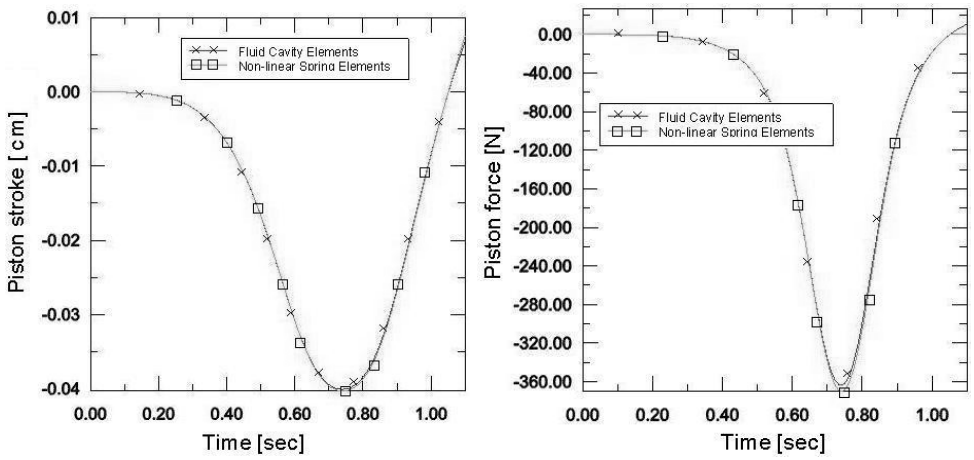

Figure 20: Fluid cavity and non-linear Spring elements comparison

4.2 Controllable piezo-valve

Airflow through the controllable valve was modelled with the equation:

$$\Delta p(c,t) = C_V(c) \cdot q(t) \tag{12}$$

Pressure difference Δp between the pneumatic cylinder and the environment is proportional to the rate of mass flow $q(t)$. The flow resistance $C_V(c)$ depends on the control variable c:

$$C_V = \begin{cases} 1.000e+19, & for\ c = -1 \quad (valve\ closed) \\ 0.155e+9\ , & for\ c = 1 \quad (valve\ open) \end{cases} \tag{13}$$

Flow resistance for the open valve was chosen so that it corresponds to the flow rate of 30 l/min at the pressure difference of 0.1 MPa.

4.3 Control strategy

The goal for the control procedure is to keep the value of piston force F_P below some critical level F_{cr}. This is achieved by means of opening the valve whenever $F_P \geq F_{cr}$ and closing it if F_P drops below the critical value. At some point during the high wind the decay sign of F_P is changed and under pressure starts to build up in the cylinder. At this point the valve is opened again in order to allow the air to flow back into the cylinder. The control procedure described above can be summarised in the diagram shown on Figure 21.

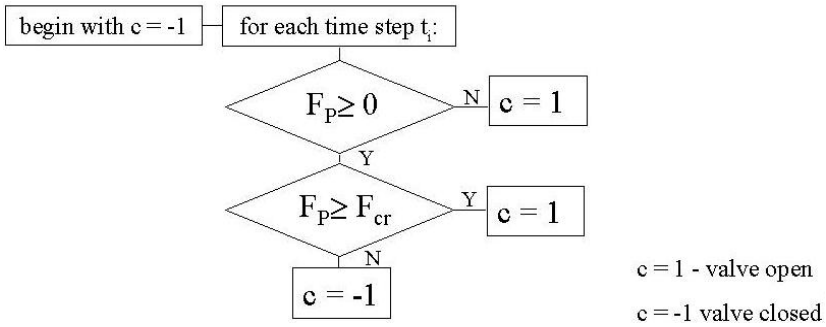

Figure 21: Control procedure

4.4 Numerical results

The use of piston strokes is depicted in Figure 22. The maximum stroke is 43.5 mm, which means 87% of the allowable strokes are used. The active phase of the process begins at the 22mm stroke approximately, that is, at about 44% of allowable strokes.

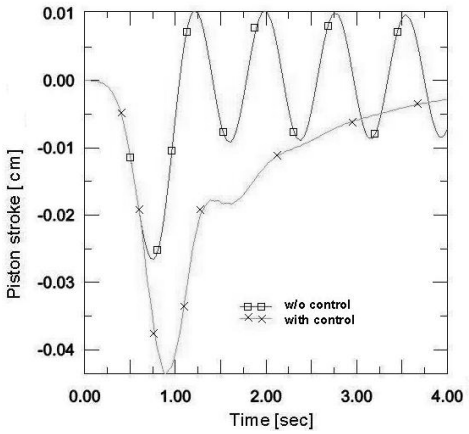

Figure 22: Piston rod displacement

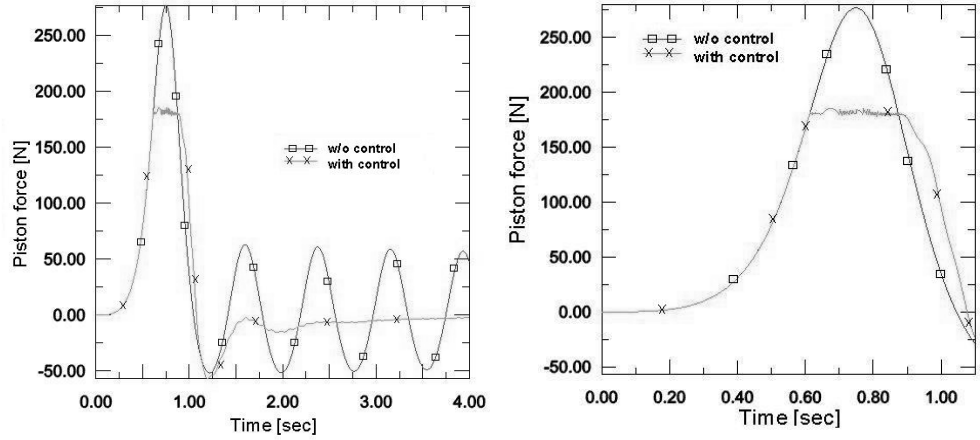

Figure 23: Dynamic force in pneumatic piston

Peak force for the reference case (w/o control) is 277 N and the critical value for the control procedure was set at 180 N. Maximum value obtained during simulation was 185 N, which means that peak dynamic force was mitigated by 35% (Fig 23). If a smaller piston force was chosen as critical, or the rising time of the blow was shorter, then the maximum force obtained during simulation would significantly exceed the critical value. Therefore, for the given increase time of the high wind, the 35% mitigation of force response obtained is about the maximum gain.

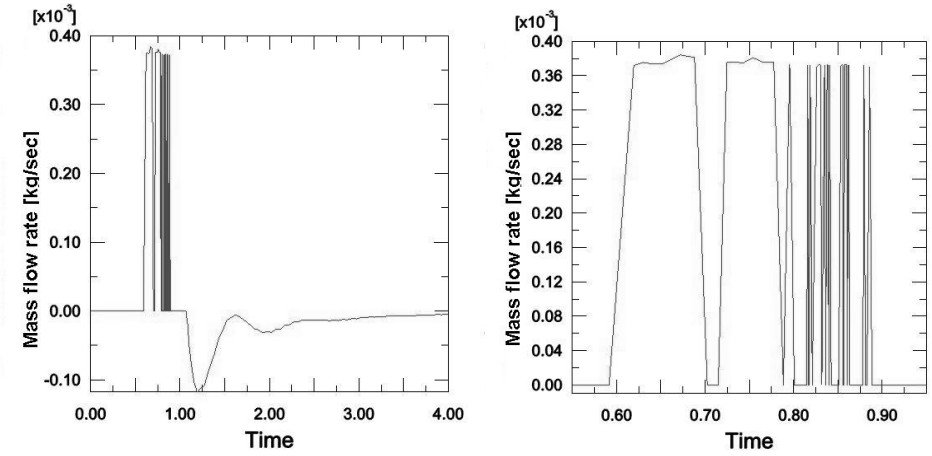

(a) (b)

Figure 24: Mass flow rate mf through the valve
(a) whole-time domain
(b) time window 0.5 – 1.0 section

Zero value on Figure 6 indicates valve closed, whereas positive values correspond to flow out of the cylinder and negative values to flow into the cylinder. It can be seen that during the peak load the valve has to stay open to prevent the force from rising, and after the biggest load intensity the valve is opened in a sequence of short impulses (Figure 24b). In the current example it is assumed that opening/closing of

the valve is instantaneous. This is a reliable assumption since the response time of the piezo-valve is of the order 1 ms. The total mass flow is calculated as:

$$mf_{TOT}(\tau) = \int_0^{\tau} mf(t)dt \tag{14}$$

where *mf(t)* is the mass flow rate, and is depicted in Figure 25. One can observe that final value is not equal to zero, which means that the amount of air in the cylinder at the end of simulation is not equal to the initial amount. Since total mass flow asymptotically approaches zero, the time required for the system to return to its initial state would be too long.

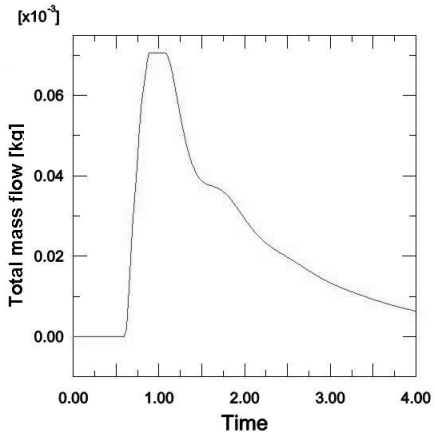

Figure 25: Total mass flow through the valve

4.5 Experimental set-up

The system shown in Figure 26 has been manufactured in order to verify numerical results. An air outlet from the cylinder was connected to the on/off valve (Figure 27). Control of the valve opening was obtained by means of Cedrat Technologies piezo-actuator. Its integral part is a mechanical amplifier of displacements which enables us to obtain displacement of 0.2 mm. The response time of such a piezo-actuated valve is less than 1ms. Initial tests indicated that the blocking force of the actuator is enough to withstand forces of magnitude considered in the numerical simulations.

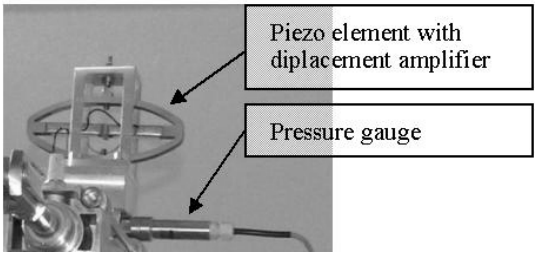

Figure 26: Cedrat Technologies piezo-actuator as an element of the controllable valve

In order to overcome the problem of a rate of flow back into the cylinder that is too slow (Figure 27) the system was additionally equipped with an air reservoir connected to the cylinder outlet. During the rising phase of the load, air from cylinder is controllably pressed to the accumulator and returned into the cylinder during the decay phase of loading. This forms a closed system which can work in sequence.

The feedback was established between the pressure transducer monitoring, the pressure/force in the cylinder and the piezo-actuator opening/closing the orifice. Set-up was integrated using the Bruel & Kjaer PULSE system.

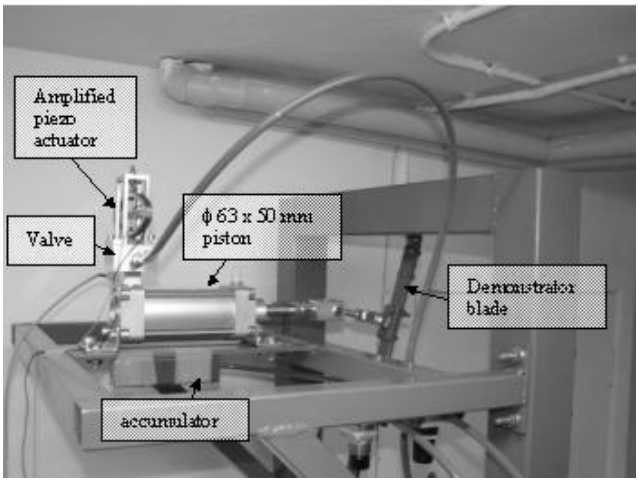

Figure 27: Experimental set-up

5 Dynamic mass identification under impact loading

An optimal strategy of structural adaptation depends on the impact load, which has to be identified in real-time. In some cases (for example, when the dropping mass is known in advance) the impact velocity measurement is sufficient to perform the desired structural adaptation. However, in many cases (for example, an unknown hitting object) on-line determination of the impact velocity as well as the mass of the hitting object is the real challenge. Having both of these parameters determined, the further optimal structural response can be performed via an open-loop control process.

In order to perform the feasibility study of a real-time dynamic mass identification technique a drop-testing stand was used. The main objective for the study was determination of the time delays in the mass identification procedure, when we assumed that the process was being performed after the beginning of the impact phenomena. The detected mass value can be used for the impact energy determination if the velocity of the falling mass was also monitored. Having the mass and velocity of the monitored object determined before the impact force reached its maximum value, it would be reasonable to apply a methodology to feed up an adaptive impact absorption system operating in real-time. The objective of this

research is to give an answer to the following question: How fast are we able to perform a mass identification after the beginning of an impact phenomenon?

5.1 Analytical model

The considered concept of the falling mass identification was analysed analytically on a simple 2 DoF model (see Figure 28a). The parameters of the model were taken close to the values present in the experimental model. The analysis, via MATLAB software, allowed us to come to the conclusion that it is feasible to identify the mass on the basis of its acceleration and impact force. The numerical experiment showed that the mass value is readable 1–2ms after impact instant (Fig. 28b) in case of concluding on the basis of mass acceleration and taking into account inertia of the system.

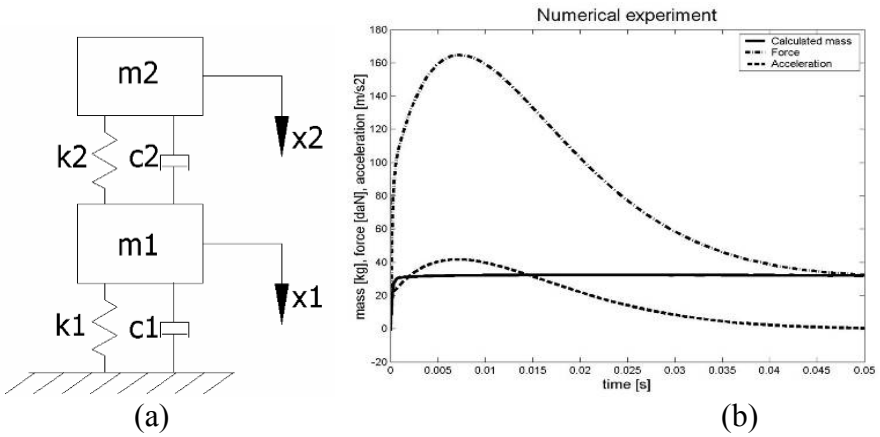

Figure 28: Numerical model (a) schema of the model and (b) results obtained

5.2 Experimental verification – drop test stand

The main parts of the drop-test stand (see Fig. 29 b) were a magneto-rheological (MR) damper (1) mounted in a vertical position, a frame and a carriage. The stand was fixed to a foundation plate in order to reduce measurement noise. The lift mechanism enabled to conduct the drop tests up to 700 mm height. The mass (2) was guided by a rail system embedded in the frame, to ensure the stability of the vertical movement. The impact of the dropped carriage took place via a rubber bumper (3) located on the impact surface.

During the tests the following signals were acquired (Fig. 29b): a force signal from a sensor fixed to a piston rod of the MR damper (4) in order to measure the full impact history; a signal from an optical switch (5) acting as a trigger and enabling determination of the horizontal speed of the carriage just before the impact. The test procedure also covered the measuring of acceleration at two points: deceleration of the falling mass (6a) and acceleration (6b) of the piston rod of the MR damper (7).

5.3 Experimental mass identification

Impact forces acquired during the experiments with several masses had characters showed in Fig 30a. The critical maximum value of the force was recorded after 9–15ms from the beginning of the phenomena dependent on the dropped mass.

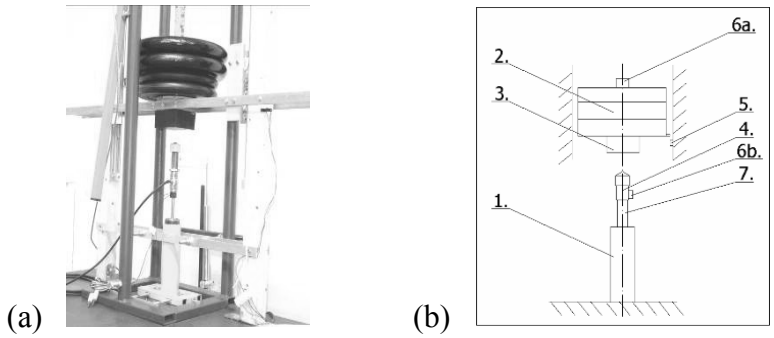

Figure 29: Drop test stand (a) general view and (b) main parts and sensors distribution

The process of mass identification was performed in two routines, one on the basis of deceleration of the falling body and the other on the basis of acceleration of the impacted body (piston rod). Accelerations measured in the two locations were characterised by curves presented in Fig 30b. In order to obtain a meaningful signal from the acceleration of the piston rod it was conditioned with a low pass filter (see Fig 30b). Results of the mass identification on the basis of the falling body deceleration were performed for a series of masses. The meaningful mass values were observable after 2-4ms from the impact instant (see Fig. 31a). Mass identification on the basis of the impacted body acceleration was performed on the basis of the filtered signal. The results of the analysis and comparison between both methods are depicted in Fig. 31b.

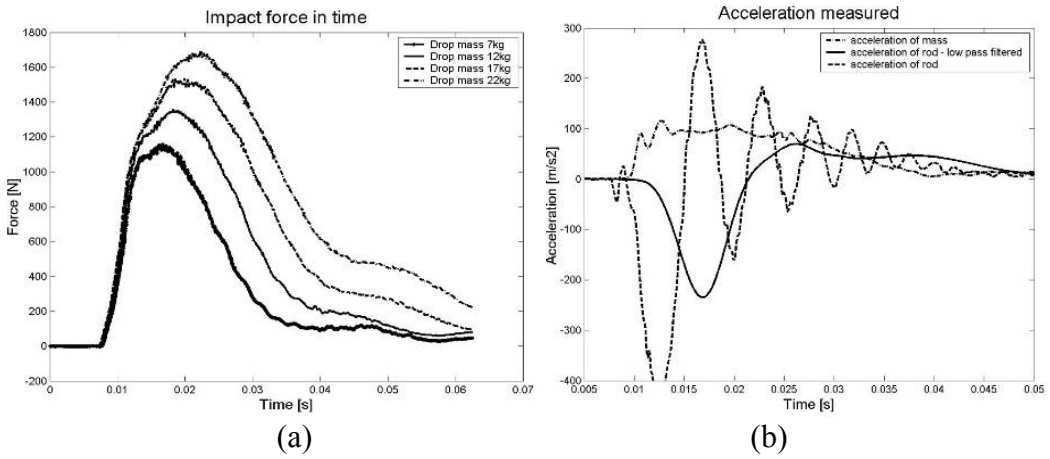

Figure 30: Measured signals for the drop test (a) force under the dissipater and (b) acceleration measured on the falling mass and top of MR damper.

Much better results of the mass identification were achieved for the case where deceleration of the falling body was used. The data enabled us to perform reliable dynamic mass identification at the beginning of the impact phenomena, much sooner than the maximum force value was observed. On the contrary, when the acceleration of the MR dumper piston was used the mass was much less reliably identified and the value was observable after 20ms from the impact instant (see Fig. 31b). It was caused by the fact that the mass identification was possible only when the falling body and piston rod moved jointly.

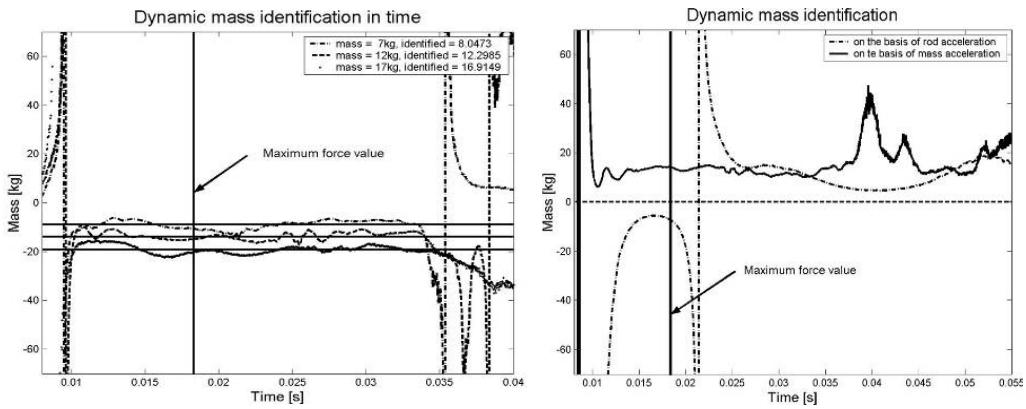

(a) (b)

Figure 31: Mass identification (a) accelerated measured on the falling mass and (b) accelerated measured on the top of MR damper

6 Conclusions

The following overall approach in design for adaptive impact absorption (AIA systems) can be proposed:

- design topological pattern (allowing large deformations in location of structural fuses) and geometry of adaptive structure for variety of all expected extreme loadings
- determine optimal yield stress level distribution (constant or time-dependent) and the corresponding dynamic responses for each expected extreme loading scenarios.
- apply in real-time the pre-computed control strategy as the response for detected and identified (via an on-line sensor system) impact.

The main challenging problems to be solved to develop the proposed methodology of design for AIA are the following:

- to develop technologies for structural fuses with short response-time
- to develop techniques of on-line impact-load identification
- to develop control algorithms for structural adaptation
- to apply integrated AIA systems to well-chosen demonstrative case studies.

Acknowledgement

This work was supported by grant No. MAT-INT PBZ-KBN-115/T08/2004, 2005-2008, funded by the National Research Committee and presents parts of the Ph.D. theses of the second, third and fourth authors, who were supervised by the first author. The authors would also like to gratefully acknowledge financial support through the 5FP EU project Research Training Networks "SMART SYSTEMS" HPRN-CT-2002-00284.

References

[1] R.R Mayer, N. Kikuchi, R.A. Scott, "Applications of Topology Optimization Techniques to Structural Crashworthiness", Int. J. Num. Meth. Engrg., vol.39, 1383-1403, (1996)

[2] A.R.Díaz, C.A. Soto, "Lattice Models for Crash Resistant Design and Optimization, Proceedings of 3rd World Congress of Structural and Multidisciplinary Optimization (WCSMO), Buffalo, New York, USA, May 17-2, (1999).

[3] K. Yuge, N. Iwai, N. Kikuchi, "Topology Optimization Algorithm for Plates and Shells Subjected to Plastic Deformations", proc. 1998 ASME Design Engineering Technical Conference, paper DET98/DAC-5603, (1998)

[4] K. Maute, S. Schwartz, E. Ramm, "Adaptive Topology Optimization of Elastoplastic Structures", Structural Optimization, 15, 81-89, (1998)

[5] J.S. Arora, C.H. Kim, A.R Mijar, "Simplified models for Automotive Crash Simulation and Design Optimization", Proceedings of 3rd WCSMO, Buffalo, New York, USA, May 17-2, (1999).

[6] H. Yamakawa, Z. Tsutsui, K. Takemae, Y. Ujita, Y. Suzuki, "Structural Optimization for Improvement of Train Crashworthiness in Conceptual and Preliminary Designs, Proc. 3rd WCSMO, Buffalo, New York, USA, May 17-2, (1999).

[7] L. Knap, J. Holnicki-Szulc, "Optimal Design of Adaptive Structures for the Best Crash-Worthiness, Proc. 3rd WCSMO, Buffalo, New York, USA, May 17-20, (1999).

[8] P. Pawlowski, M. Wiklo, J. Holnicki-Szulc, Optimal Strategies of Adaptive Impact Absorption", in Proc. 5th WCSMO, Lido di Jesolo, July 2003

[9] P. Pawlowski, J. Holnicki-Szulc, "Adaptive Structures under Extreme Loads", proc. 3rd European Conference on Structural Control, Vienna, July 2004.

[10] A. Mroz, J. Holnicki-Szulc, „Semi-Active Control of Wind Impact effects by Means of Pneumatic System", Proc. NNMAE Conference, Thessalonica, July 2006.

[11] K. Sekula, G. Mikułowski, J. Holnicki-Szulc, „Real-Time Dynamic Mass Identification", in Proc. 3rd European Workshop on Structural Health Monitoring, Granada, 2006.

[12] Jan Holnicki-Szulc (Ed.) „Smart Technologies for Structural Safety", J.Wiley, 2007, in preparation

[13] EU Project ADLAND IST-FP6-2002-2006, http://smart.ippt.gov.pl/adland/.
[14] EU Project UPWIND FP6-ENERGY-2006, http://www.duwind.tudelft.nl/
[15] G. Belforte, S. Mauro, G. Mattiazzo, "A method for increasing the dynamic performance of pneumatic servosystems with digital valves". Mechatronics 14, (2004), 1105-1120.
[16] Ch. Mao-Hsiung, Ch. Chung-Chieh, T. Tan-Ni, "Large stroke and high precision pneumatic-piezoelectric hybrid positioning control using adaptive discrete variable structure control", Mechatronics 15, (2005), 523-545.